

# Dynamic elastic analysis of pile foundations using finite element method in the frequency domain

Guoxi Wu and W.D. Liam Finn

**Abstract:** A quasi-three-dimensional finite element method of analysis is proposed for the dynamic response analysis of pile foundations that is computationally feasible for practical applications. The method uses a simplified three-dimensional wave equation for describing the dynamic response of the soil. The response of the pile foundation is computed directly without having to use pile-soil-pile interaction factors. The quasi-three-dimensional solution greatly reduces the computational time for the direct analysis of pile groups. The method is presented here for an elastic response so that it can be validated against existing more exact elastic solutions and low-amplitude field vibration tests. The method is extended to nonlinear dynamic response analysis in an accompanying paper.

*Key words:* piles, dynamics, quasi-three-dimensional, impedances, finite element.

**Résumé :** Une méthode d'éléments finis quasi-tridimensionnelle est proposée pour analyser la réponse dynamique des pieux dans des conditions de calcul compatibles avec les applications pratiques. La méthode utilise une équation d'onde simplifiée à trois dimensions pour décrire la réponse dynamique du sol. La réponse du pieu est calculée directement sans avoir à utiliser les coefficients d'interaction pieu-sol-pieu. La solution quasi-tridimensionnelle réduit fortement le temps de calcul nécessaire pour l'analyse directe des groupes de pieux. On présente ici la méthode pour une réponse élastique de façon à pouvoir la valider par rapport à des solutions élastiques plus exactes et à des résultats d'essais de vibration à faible amplitude en place. La méthode est étendue à l'analyse de la réponse dynamique non-linéaire dans un article joint.

*Mots clés:* pieux, dynamique, quasi-tridimensionnel, impédances, éléments finis.  
[Traduit par la rédaction]

## Introduction

The objective of this paper is to present a new method for the direct dynamic analysis of pile foundations. It is based on a simplified formulation of the three-dimensional (3D) response under dynamic excitation (Wu 1994; Finn and Wu 1994; Wu and Finn 1995). The method is developed in this paper for elastic conditions so that existing elastic solutions may be used to check the accuracy and reliability of the method. The method has been extended to nonlinear response in an accompanying paper.

Kaynia and Kausel (1982) have provided elastic solutions for a number of different pile groups based on boundary-integral techniques. In addition they have provided dynamic interaction factors that are used to generate a pile group response from a single pile response, as in the DYNA3 method of analysis which is widely used in practice (Novak et al. 1990). The Kaynia and Kausel (1982) data are used to validate the elastic solutions derived using the quasi-3D method of analysis.

The method has also been tested under field conditions. It has been used to analyze the small amplitude forced vibration test of a full-scale Franki pile described by Sy and Siu (1992)

and the free vibration of a transformer bank on a six-pile foundation. This later test was conducted by Crouse and Cheang (1987) on the transformer bank at Duwamish Substation in Seattle, Washington, U.S.A.

The proposed method gave results that agreed adequately with both analytical and field data.

## Lateral dynamic analysis of pile foundations

Under vertically propagating shear waves (Fig. 1) the foundation soils undergo mainly shearing deformations in the  $XOY$  plane, except in the area near the pile where extensive compression deformations develop in the direction of shaking. The compressive deformations also generate shearing deformations in the  $YOZ$  plane, as shown in Fig. 1. In the light of these observations, assumptions are made that the dynamic motions are governed by shear waves in the  $XOY$  and  $YOZ$  planes, and compression waves in the shaking direction,  $Y$ . Deformations in the vertical direction and normal to the direction of shaking are neglected.

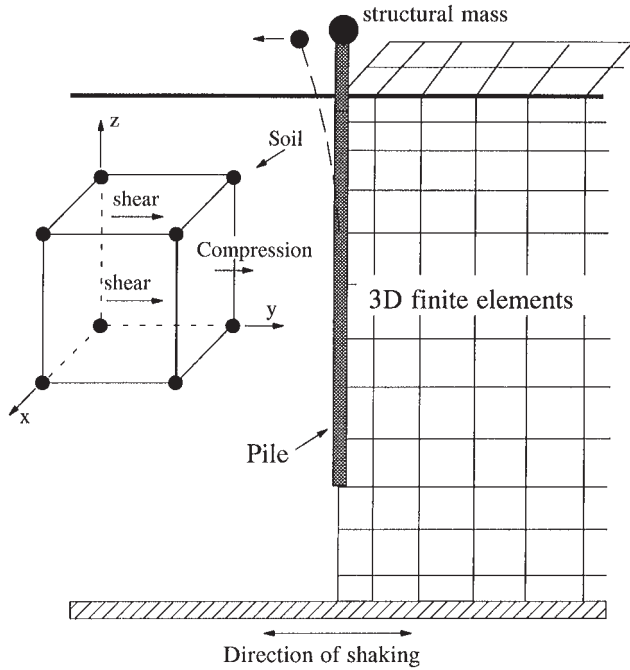
Let  $v$  represent the displacement of soil in the shaking direction,  $Y$ . Then the compression force per unit volume is  $\theta G^* \partial^2 v / \partial y^2$ . The shear forces per unit volume in the  $XOY$  and  $YOZ$  planes are  $G^* \partial^2 v / \partial z^2$  and  $G^* \partial^2 v / \partial x^2$ , respectively. The two shear waves propagate in the  $Z$  direction and  $X$  direction, respectively. The inertial force per unit volume is  $\rho_s \partial^2 v / \partial t^2$ . Applying dynamic force equilibrium in the  $Y$  direction, the

Received February 17, 1996. Accepted October 8, 1996.

**G. Wu.** AGRA Earth & Environmental Ltd., 2227 Douglas Road, Burnaby, BC V5C 5A9, Canada.

**W.D.L. Finn.** Department of Civil Engineering, The University of British Columbia, Vancouver, BC V6T 1Z4, Canada.

**Fig. 1.** The principle of the quasi-3D dynamic analysis of pile–soil–structure interaction.



governing equation describing the free vibration of the soil continuum is written as

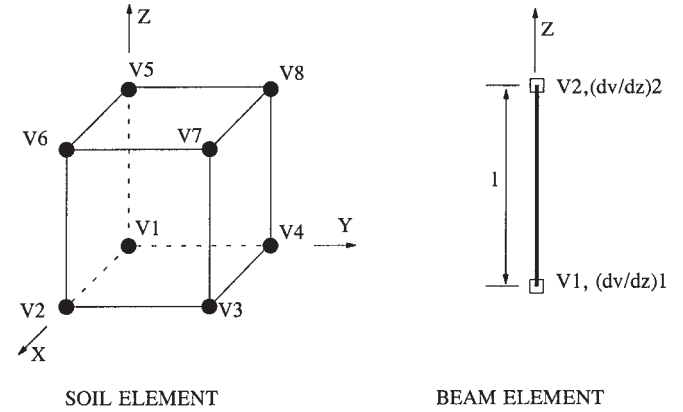
$$[1] \quad \rho_s \frac{\partial^2 v}{\partial t^2} = G^* \frac{\partial^2 v}{\partial x^2} + \theta G^* \frac{\partial^2 v}{\partial y^2} + G^* \frac{\partial^2 v}{\partial z^2}$$

where  $\rho_s$  is the mass density of soil, and  $G^*$  is the complex shear modulus. The complex shear modulus  $G^*$  is expressed as  $G^* = G(1 + i2\lambda)$ , in which  $G$  is the shear modulus of soil,  $\lambda$  is the strain-dependent damping ratio equivalent to the hysteretic damping ratio of the soil, and  $i = (-1)^{1/2}$ . The parameter  $\theta$  is given by  $\theta = 2/(1 - \mu)$  assuming plane strain conditions in the direction of shaking (Wu 1994; Wu and Finn 1996), and  $\mu$  is the Poisson's ratio of the soil. Free horizontal displacement is allowed at the lateral boundaries of the finite element model.

Piles are modelled using the ordinary Eulerian beam theory. The basic parameters for modelling the bending behaviour of the pile are the density  $\rho_p$ , sectional area  $A_p$ , and the flexural rigidity  $E_p I_p$ . Only the bending motion in the plane of shaking ( $Y$  direction) is considered. In the case of a pile group, the rocking stiffness due to the vertical resistances of the individual piles is also considered. The analysis of rocking is presented in a later section.

Radiation damping represents dissipation of vibration energy through the boundaries of the finite element model into the semi-infinite soil medium. The loss of energy due to radiation damping can be modelled by using energy transmitting boundaries or by applying dashpots to the pile shaft. The use of dashpots is selected herein because of its simplicity and the fact that its effectiveness has been verified by Gazetas et al. (1993). The reflecting waves from the free-displacement boundaries are expected to be absorbed by the radiation damping and the hysteretic damping of soil. The velocity proportional damping force  $F_d$  per unit length along the pile is given by

**Fig. 2.** Finite element compositions for modelling horizontal motions.



$$[2] \quad F_d = c_x \frac{dv}{dt}$$

where  $c_x$  is the radiation dashpot coefficient for horizontal motion. A simple approximate expression for the radiation dashpot coefficient  $c_x$ , proposed by Gazetas et al. (1993), is adopted in the analysis. This expression is written as

$$[3] \quad c_x = 6.0 \rho_s V_s d \left( \frac{\omega d}{V_s} \right)^{-0.25}$$

in which  $V_s$  is the shear wave velocity of the soil,  $d$  is diameter of the pile, and  $\omega$  is the excitation frequency of the external load.

The general partial differential equations are then discretized using the finite element theory. An eight-node brick element is used to model the soil, and a two-node beam element is used to model the pile (Fig. 2). At each soil node, nodal displacement is permitted only in the direction of shaking,  $Y$ . Both translational displacement and rotational degrees of freedom are used to model the bending behaviour of the pile.

Using the standard procedures of the finite element method, the global dynamic equilibrium equations are written in matrix form as

$$[4] \quad [M^*] \left\{ \frac{\partial^2 v}{\partial t^2} \right\} + [C^*] \left\{ \frac{\partial v}{\partial t} \right\} + [K^*] \{v\} = \{P(t)\}$$

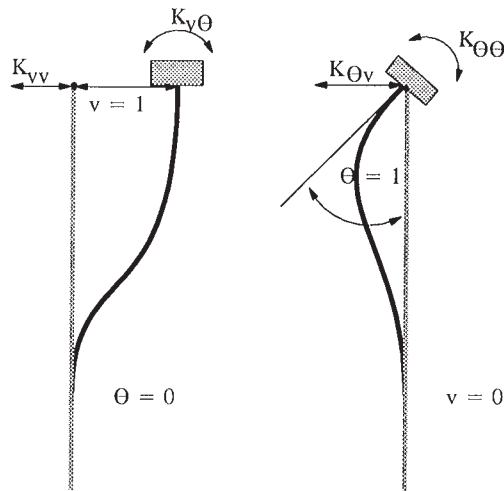
in which  $P(t)$  is the external dynamic load vector, and  $\{\partial^2 v / \partial t^2\}$ ,  $\{\partial v / \partial t\}$ , and  $\{v\}$  are the relative nodal acceleration, velocity, and displacement, respectively.  $[M^*]$ ,  $[C^*]$ , and  $[K^*]$  are the mass, damping, and stiffness matrices of the soil–pile system vibrating in the horizontal direction.  $[K^*]$  is a complex stiffness matrix that includes the hysteretic damping of the soil.

### Lateral pile head impedances

The impedances  $K_{ij}$  are defined as the complex amplitudes of harmonic forces (or moments) that have to be applied at the pile head in order to generate a harmonic motion with a unit amplitude in the specified direction (Novak 1991). The concept of translational and rotational impedances is illustrated in Fig. 3. The translational, the cross-coupling, and the rotational impedances of the pile head are represented by  $K_{vv}$ ,  $K_{v\theta}$ , and  $K_{\theta\theta}$ , respectively.

Since the pile head impedances  $K_{vv}$ ,  $K_{v\theta}$ , and  $K_{\theta\theta}$  are complex valued, they are usually expressed by their real and imaginary parts as

Fig. 3. Pile head impedances.



$$[5] \quad K_{ij} = k_{ij} + iC_{ij} \quad \text{or} \quad K_{ij} = k_{ij} + i\omega c_{ij}$$

in which  $k_{ij}$  and  $C_{ij}$  are the real and imaginary parts of the complex impedances, respectively;  $c_{ij} = C_{ij}/\omega$  is the coefficient of equivalent viscous damping; and  $\omega$  is the circular frequency of the applied load.  $k_{ij}$  and  $C_{ij}$  are usually referred to as the stiffness and damping at the pile head. All the parameters in eq. [5] are dependent on the frequency  $\omega$ .

Pile head impedances are evaluated as functions of excitation frequency by subjecting the system to harmonic loads. If  $\{P(t)\} = \{P_0\} e^{i\omega t}$  and the steady-state displacement vector  $\{v\} = \{v_0\} e^{i\omega t}$ , eq. [4] therefore takes the form

$$[6] \quad [K]_{\text{global}} \{v_0\} = \{P_0\}$$

Where  $[K]_{\text{global}}$  is a complex valued matrix given by

$$[7] \quad [K]_{\text{global}} = [K^*] + i\omega[C^*] - \omega^2[M^*]$$

When displacement conditions are imposed at the pile head to determine pile head impedance, the corresponding forces (shears and moments) at the pile head can be determined using eq. [6].

### Vertical dynamic analysis of pile foundations

Under a vertically propagating compression wave, the soil medium mainly undergoes compressive deformations in the vertical direction. In the two horizontal directions, shearing deformations are generated due to the internal friction of the soil. Although compressions occur in the two horizontal directions, assumptions are made that the normal stresses in the two horizontal directions due to vertical excitation are small and can be ignored. Therefore the dynamic motions of the soil are governed by the compression wave in the vertical direction and the shear waves propagating in the two horizontal directions  $X$  and  $Y$ .

Analogous to the governing equation in the horizontal direction, the quasi-3D wave equation of soil in the vertical direction is given by

$$[8] \quad \rho_s \frac{\partial^2 w}{\partial t^2} = G^* \frac{\partial^2 w}{\partial x^2} + G^* \frac{\partial^2 w}{\partial y^2} + \theta_z G^* \frac{\partial^2 w}{\partial z^2}$$

where  $w$  is the soil displacement in the vertical direction. The parameter  $\theta_z$  is given by  $\theta_z = 2(1 + \mu)$  based on equilibrium of

the model in the vertical direction. Again, the radiation damping resulting from waves travelling away from the pile group is accounted for by using velocity proportional damping along the pile shaft. The damping force  $F_{dz}$  per unit length along the pile is given by

$$[9] \quad F_{dz} = c_z \frac{dw}{dt}$$

where  $c_z$  is the radiation dashpot coefficient for vertical motion. A simple approximate expression for the radiation dashpot coefficient  $c_z$  proposed by Gazetas et al. (1993) is adopted in the analysis. This expression is written as

$$[10] \quad c_z = \rho_s V_s d \left( \frac{\omega d}{V_s} \right)^{-0.25}$$

in which  $V_s$  is the shear wave velocity of the soil,  $d$  is the diameter of the pile, and  $\omega$  is the excitation frequency of the external load.

Following the general procedures used in the finite element method, the global dynamic equilibrium equations are written in matrix form as

$$[11] \quad [M_z^*] \left\{ \frac{\partial^2 w}{\partial t^2} \right\} + [C_z^*] \left\{ \frac{\partial w}{\partial t} \right\} + [K_z^*] \{w\} = \{P_z(t)\}$$

in which  $P_z(t)$  is the external dynamic load vector, and  $\{\partial^2 w/\partial t^2\}$ ,  $\{\partial w/\partial t\}$ , and  $\{w\}$  are the relative nodal acceleration, velocity, and displacement, respectively.  $[M_z^*]$ ,  $[C_z^*]$ , and  $[K_z^*]$  are the mass, damping, and stiffness matrices of the soil-pile system vibrating in the vertical direction.  $[K_z^*]$  is normally a complex matrix.

### Rocking impedances of pile groups

The rocking impedance of pile group is a measure of the complex resistance to rotation of the pile cap due only to the resistance of each pile in the group to vertical displacements. The rocking impedance  $K_{rr}$  of a pile group is defined as the summation of the moments of the axial pile forces around the centre of rotation of the pile cap for a harmonic rotation with unit amplitude at the pile cap. This definition is quantitatively expressed as

$$[12] \quad K_{rr} = \sum r_i F_i$$

where  $r_i$  is the distance between the centre of rotation and the pile head centres, and  $F_i$  is the amplitude of axial forces at the pile heads, as shown in Fig. 4.

In the analysis, the pile cap is assumed to be rigid. For a unit rotation of the pile cap, the vertical displacements  $w_i^p$  at all pile heads are determined according to their distances from the centre of rotation  $r_i$ .

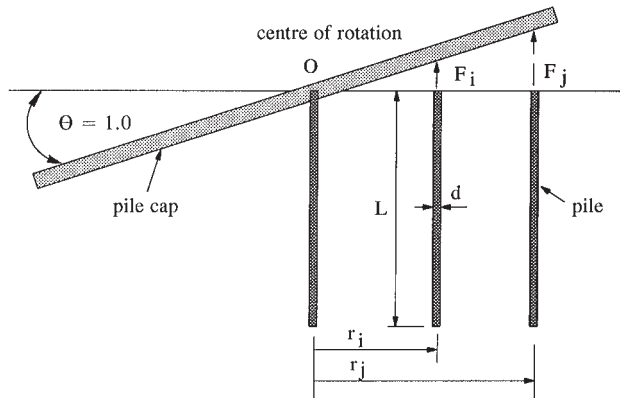
For a given combination of vertical displacement  $w_i^p$  at the pile heads, the corresponding axial forces  $F_i$  at these pile heads are determined from eq. [11]. The rocking impedance of a pile group is then computed according to eq. [12].

### Theoretical verification of model: single piles

#### Pile head impedances

To assess the accuracy of the proposed quasi-3D finite element approach, the impedance functions for single piles are

**Fig. 4.** The mechanism of rocking in a pile group.



determined and compared with the results obtained by Kaynia and Kausel (1982) using the boundary-integral method. Analyses were performed in the frequency domain for elastic conditions. Following Kaynia and Kausel, the normalized dynamic impedances  $K_{vv}/(E_s d)$ ,  $K_{v\theta}/(E_s d^2)$ , and  $K_{\theta\theta}/(E_s d^3)$  will be computed as functions of the dimensionless frequency  $a_0$ , where  $a_0$  is defined as

$$[13] \quad a_0 = \frac{\omega d}{V_s}$$

in which  $\omega$  is the angular frequency of the applied loads (force and moment) at the pile head,  $d$  is the diameter of the pile, and  $V_s$  is the shear wave velocity of the soil medium. For a uniform profile with a shear modulus  $G$  and a mass density  $\rho$ ,  $V_s$  is computed as  $V_s = (G/\rho)^{0.5}$ .

Kaynia and Kausel give the dynamic impedances for a single pile for the case when  $E_p/E_s = 1000$ , where  $E_p$  and  $E_s$  are the Young's moduli of the pile and the soil, respectively. Other parameters used in their analysis are a Poisson's ratio  $\mu = 0.4$ , a hysteretic damping ratio  $\lambda = 5\%$ , and the mass density ratio  $\rho_p/\rho_s = 1.4$ . The finite element modelling of the system used in the present analysis is shown in Fig. 5.

The computed normalized stiffness and associated damping factors for translational and rotational degrees of freedom expressed as a function of frequency are compared with those of Kaynia and Kausel (1982) in Figs. 6 and 7, respectively. The dynamic impedances from the quasi-3D analysis agree well with those of Kaynia and Kausel. The computed quantities are slightly smaller than those by Kaynia and Kausel, which implies their modelling of the pile-soil systems results in a stiffer system. The comparison has been made in the frequency range  $a_0 < 0.3$ , which is representative of earthquake loading. For higher frequencies associated with vibration of machine foundations, a much finer mesh would be necessary.

It is also interesting to compare the quasi-3D results with solutions from the DYNA3 program by Novak et al. (1990), which is widely used in practice. DYNA3 uses a plane strain model developed by Novak (1974) for analysis of single piles and includes dynamic interaction factors for analysis of pile groups.

The plane strain model (Novak 1974) does not provide valid solutions for nondimensional frequencies  $a_0 < 0.3$ . At frequencies below 0.3, the dynamic stiffness computed by using the plane

**Fig. 5.** Finite element modelling of single pile for computing impedances.

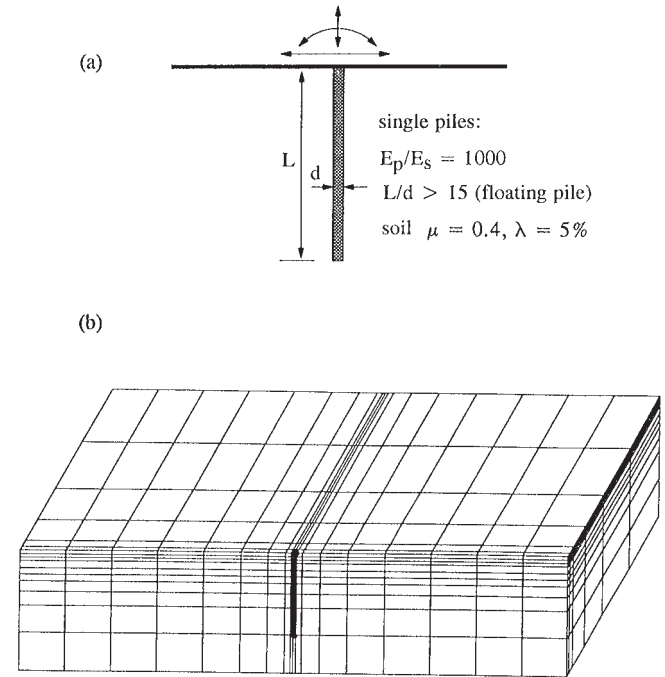
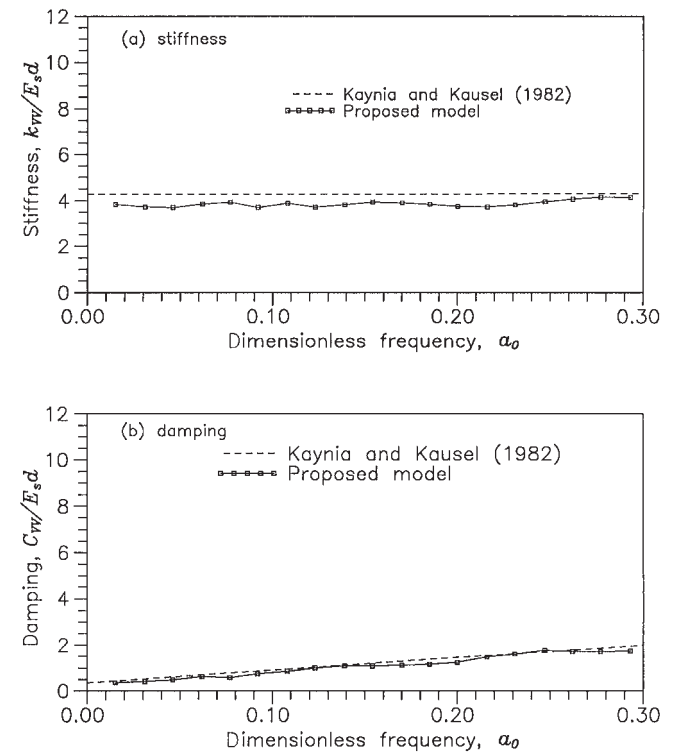


**Fig. 6.** Normalized stiffness  $k_{vv}$  and damping  $C_{vv}$  versus  $a_0$  for single piles ( $E_p/E_s = 1000$ ,  $\mu = 0.4$ ,  $\lambda = 5\%$ ).



strain model decreases steeply with a decrease in frequency, a result shown to be incorrect by Novak and Aboul-Ella (1978). Therefore, in DYNA3 the stiffnesses computed at  $a_0 = 0.3$  are used over the entire frequency range from  $a_0 = 0$  to  $a_0 = 0.3$ . This is the important frequency range for earthquake problems.

**Fig. 7.** Normalized stiffness  $k_{\theta\theta}$  and damping  $C_{\theta\theta}$  versus  $a_0$  for single piles ( $E_p/E_s = 1000$ ,  $\mu = 0.4$ ,  $\lambda = 5\%$ ).

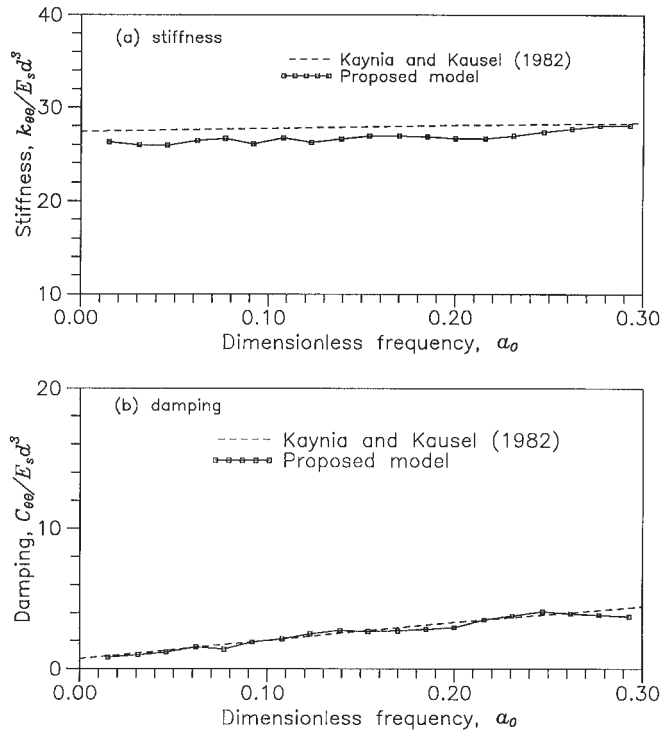
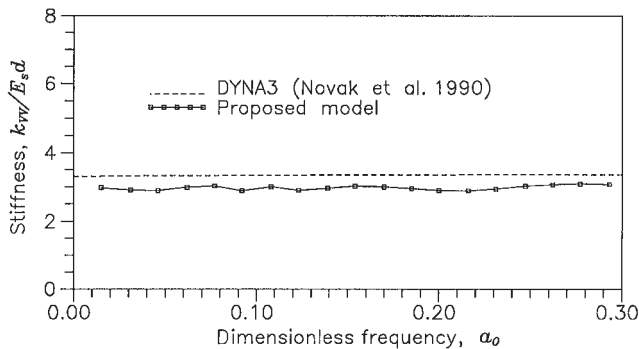


**Fig. 8.** Comparison of stiffness  $k_{vv}$  with solutions from DYNA3 (Novak et al. 1990) ( $E_p/E_s = 295$ ,  $\mu = 0.4$ ,  $\lambda = 5\%$ ).

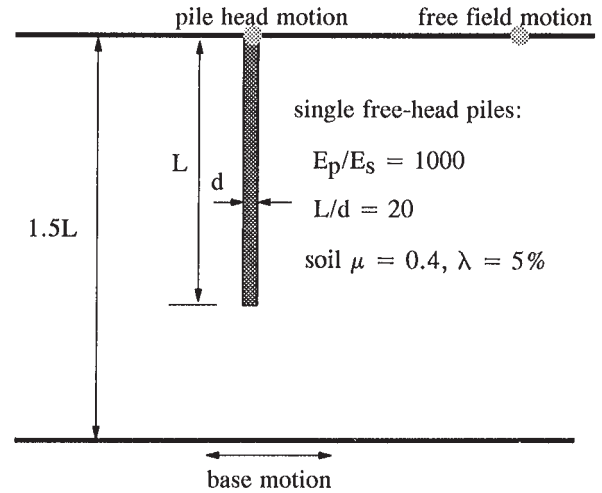


Comparison of the computed stiffnesses in this frequency range for the example problem with  $E_p/E_s = 295$  using the quasi-3D method with the approximation to the stiffnesses in DYNA3 suggests that the DYNA3 approximation is adequate for practical purposes (Fig. 8).

**Kinematic interaction**

A pile-soil system shown in Fig. 9 is subjected to a harmonic displacement  $v_b e^{i\omega t}$  at its rigid base. The dynamic response at the pile head may be same as or very close to the dynamic response at the free field surface if the pile is very flexible. However, in many cases the dynamic response at the pile head differs significantly from the response at the free field surface because piles are generally much stiffer than soil and thus

**Fig. 9.** Pile foundation for analysis of kinematic response.



modify soil deformations. This type of interaction between piles and soils is called kinematic interaction.

Let the harmonic displacements at the free field surface be represented by  $v_{ff} e^{i\omega t}$ , and at the pile head by  $v_p e^{i\omega t}$  and  $\phi_p e^{i\omega t}$ , in which  $v_p$  and  $\phi_p$  are the complex amplitudes of the translational displacement and the rotational displacement, respectively.

Absolute values of complex amplitudes of harmonic displacements are used for determining the kinematic interaction factors. The kinematic interaction factors  $I_u$  and  $I_\phi$  are defined after Gazetas (1984) as

$$[14] \quad I_u = \frac{U_p}{U_{ff}} \quad \text{and} \quad I_\phi = \frac{\Phi_p d}{U_{ff}}$$

in which  $U_p$ ,  $U_{ff}$ , and  $\Phi_p$  are the absolute values of the complex amplitudes  $v_p$ ,  $v_{ff}$ , and  $\phi_p$ , respectively; and  $d$  is the diameter of the pile.

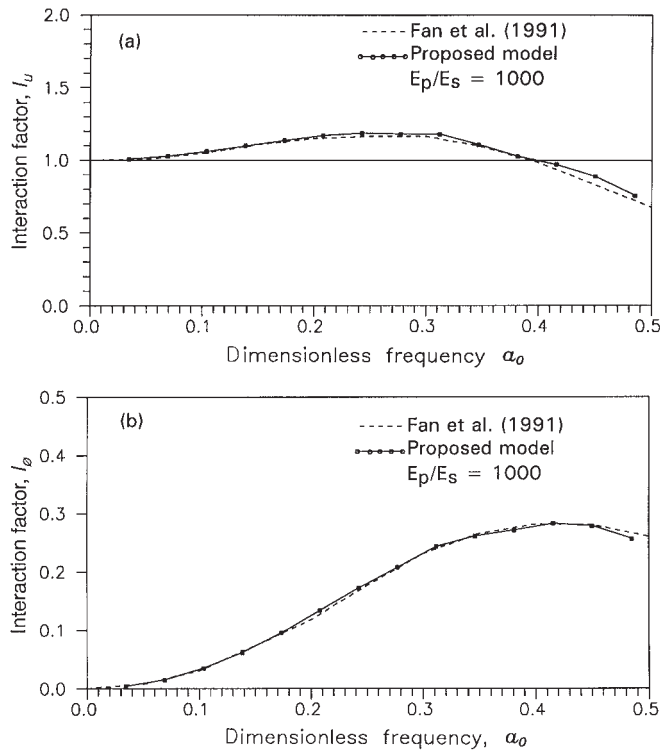
The kinematic interaction factors are obtained for a pile-soil system with a  $E_p/E_s$  ratio of 1000. The accuracy of the quasi-3D finite element method is checked against results obtained by Fan et al. (1991) using the boundary-integral method of Kaynia and Kausel(1982). The kinematic interaction factors  $I_u$  and  $I_\phi$  obtained using the proposed model are plotted in Fig. 10 as a function of the dimensionless frequency  $a_0$  together with the interaction factors obtained by Fan et al. (1991). A comparison of the two sets of factors shows that there is very good agreement between the quasi-3D solutions and the boundary element solutions.

**Theoretical verification of the model: pile groups**

The lateral impedance  $K_{vv}$  and the rocking impedance  $K_{rr}$  of a four-pile group with a pile spacing  $s$  from centre to centre of five pile diameters  $d$ ,  $s/d = 5$ , are evaluated using the proposed model. The rotational impedance  $K_{\theta\theta}$  at the head of each pile is also obtained. The properties of the pile and soil given in Fig. 5 were used in the analysis. The pile cap is rigid and rigidly connected to the pile heads.

To show the pile group effect, dynamic impedances of the pile group are normalized to the static stiffness of the pile group expressed as the stiffness of a single pile times the

**Fig. 10.** Kinematic interaction factors versus  $\alpha_0$  for  $E_p/E_s = 1000$  (soil  $\mu = 0.4, \lambda = 5\%$ ).



number of piles in the group. This normalized lateral impedance of the pile group,  $\alpha_{vv}$ , is the dynamic interaction factor for lateral loading for the given pile head conditions and is defined as

$$[15] \quad \alpha_{vv} = \frac{K_{vv}}{N k_{vv}^0}$$

where  $k_{vv}^0$  is the static lateral stiffness of an identical single pile placed in the same soil medium, and  $N$  is the number of piles in the pile group ( $N = 4$  for a four-pile group). The computed lateral interaction factors for stiffness and damping are compared with those by Kaynia and Kausel (1982) in Figs. 11a and 11b, respectively. There is good agreement between both sets of factors.

Because the piles are rigidly connected to the pile cap at the pile heads, the total rotational impedance of the pile cap  $K_{\theta\theta}^{cap}$  consists of both the rocking impedance  $K_{rr}$  of the pile group and the summation of the rotational impedances,  $K_{\theta\theta}$ , at the head of each pile

$$[16] \quad K_{\theta\theta}^{cap} = K_{rr} + \sum K_{\theta\theta}$$

The total rotational impedance of the pile cap  $K_{\theta\theta}^{cap}$  is normalized as  $K_{\theta\theta}^{cap}/(N \sum r_i^2 k_{zz}^0)$ , in which  $k_{zz}^0$  is the static vertical stiffness of an identical single pile placed in the same soil medium. The computed rotational interaction factors for stiffness and damping are compared with those by Kaynia and Kausel (1982) in Figs. 12a and 12b, respectively. The results obtained using the quasi-3D model are quite satisfactory.

**Fig. 11.** Comparison of dynamic interaction factors  $\alpha_{vv}^k$  for stiffness and  $\alpha_{vv}^c$  for damping with solution by Kaynia and Kausel for  $2 \times 2$  pile groups ( $E_p/E_s = 1000, s/d = 5.0$ ). (Note:  $\alpha_{vv} = \alpha_{vv}^k + i\alpha_{vv}^c$ )

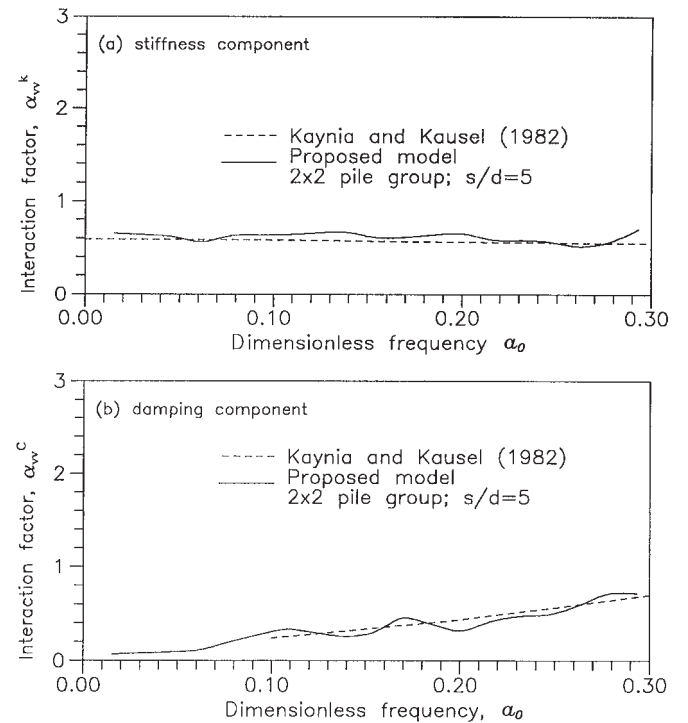


**Fig. 12.** Comparison of normalized rotational impedance of the pile cap  $K_{\theta\theta}^{cap}/A$  with solution by Kaynia and Kausel for  $2 \times 2$  pile groups ( $E_p/E_s = 1000, s/d = 5.0, A = N \sum r_i^2 k_{zz}^0$ ).

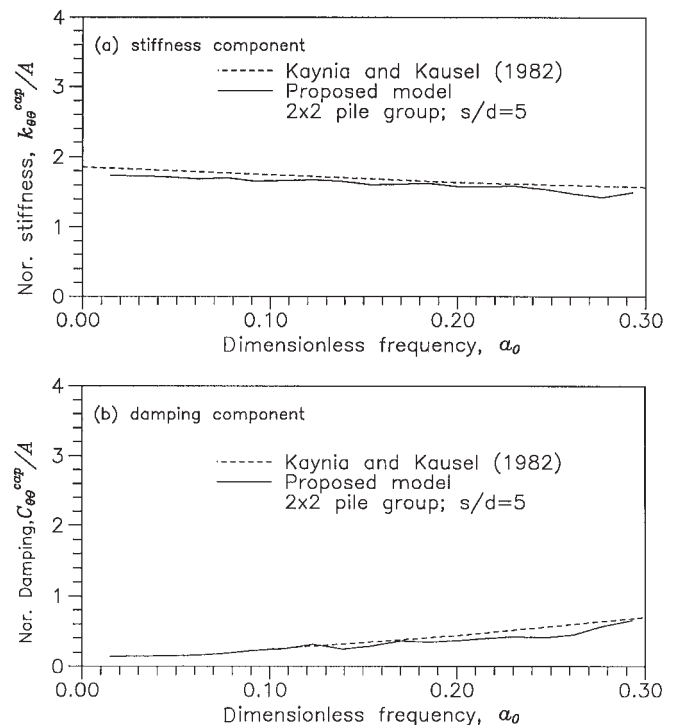
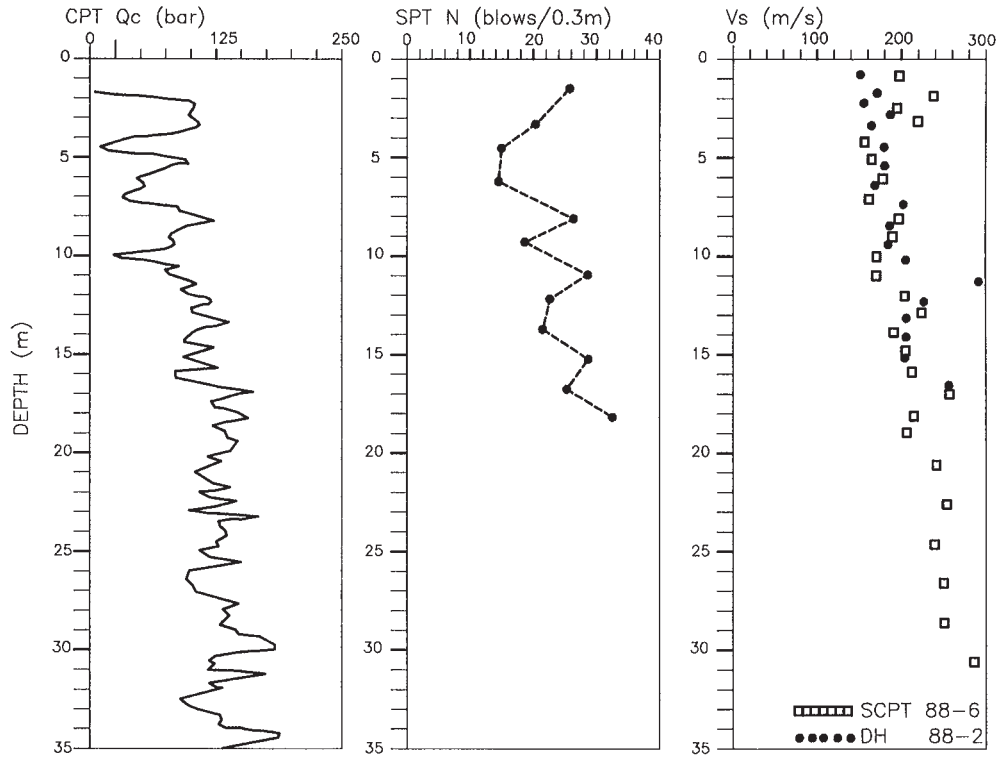


Fig. 13. The in situ measured geotechnical data (modified from Sy and Siu (1992)).



## Verification of model by field tests

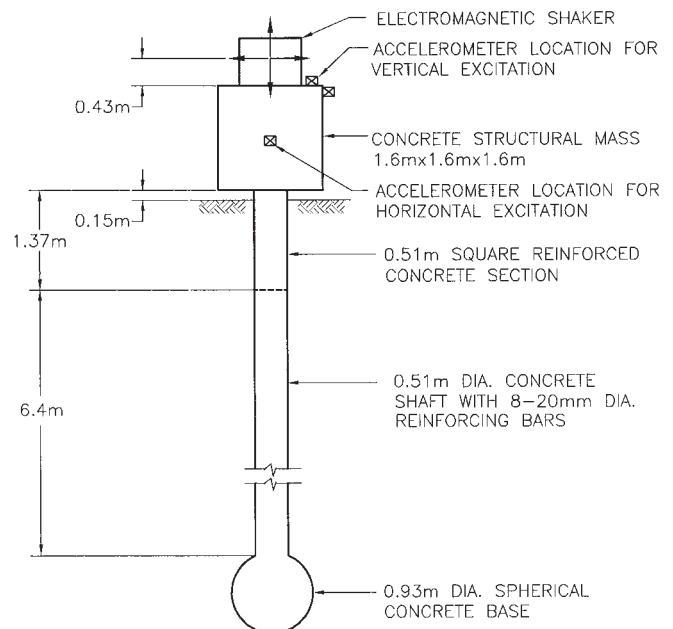
### Vibration test on a Franki pile

A full-scale vibration test on a single Franki type pile was performed by Sy and Siu (1992) in the Fraser River Delta just south of Vancouver, B.C. The soil profile at the testing site consisted of 4 m of sand and gravel fill overlaying a 1 m thick silt layer over fine-grained sand to a depth of 40 m. A seismic cone penetration test (SCPT 88-6) was conducted 0.9 m from the test pile. In addition, SPT tests were conducted in a mudrotary drill hole (DH88-2) 2.4 m from the test pile. The measured in situ shear wave velocity data are presented in Fig. 13, together with the data from the cone penetration test (CPT) and the standard penetration test (SPT).

The instrumented test pile is located as shown in Fig. 14. The pile has an expanded spherical base with a nominal diameter of 0.93 m. For 6.4 m above the expanded base, the pile has a nominal diameter of 0.51 m. The remaining length has a square cross section with a side width of 0.51 m. A structural mass consisting of a 1.6 m cube of reinforced concrete was formed on top of the pile with a clearance of 0.15 m above the ground surface.

Accelerometers were mounted on the shake mass and the pile cap to measure the dynamic input force and the pile cap responses, as shown in Fig. 14. The vertical and coupled horizontal and rocking modes of vibration were obtained by rotating the shaker so that the dynamic forces were applied in both vertical and horizontal directions. The modal frequencies of the cap-pile-soil system were estimated by applying random bandwidth excitation. Then a detailed sinusoidal frequency sweep was carried out around the natural frequency indicated from the random bandwidth test to define the resonant

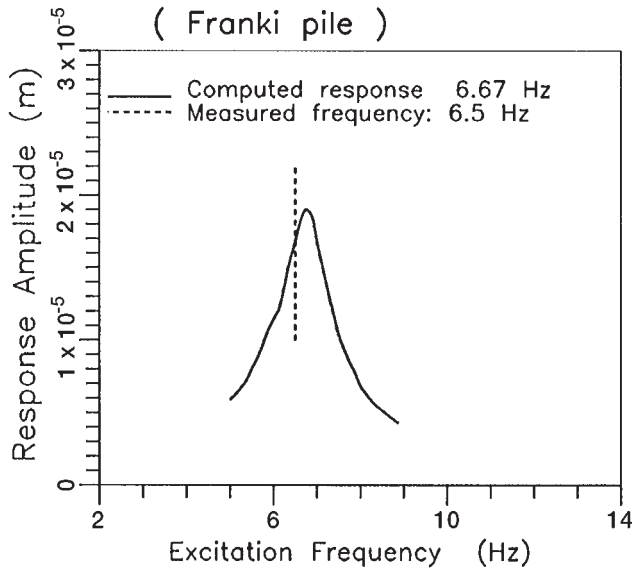
Fig. 14. The layout of the full-scale vibration test on a single pile (modified from Sy and Siu (1992)).



frequencies. The damping ratios were calculated by Sy and Siu (1992) from the measured frequency response curves.

The structural properties of the pile cap and the test pile and the distribution of shear wave velocity  $V_s$ , unit weight  $\gamma$ , and damping ratio  $D_s$  in the foundation soils used in the analysis were those given by Sy and Siu (1992). The 3D finite element model consists of 1225 nodes and 889 elements. Due to space

**Fig. 15.** Amplitudes of horizontal displacement at the centre of gravity of the pile cap versus the excitation frequency (first mode).



limitation, the detailed mesh is not shown here but can be found in Wu (1994) and is somewhat similar to the mesh shown in Fig. 5. In the mesh there is one beam element above the ground surface to represent the pile segment above the ground. The expanded base is modelled by a solid element rather than a beam element in the finite element analysis.

The frequency response analysis of the pile for the specified conditions was conducted at different frequencies  $\omega$  using a harmonic load of 165 N at the pile cap as specified by Sy and Siu (1992). The computed horizontal displacement amplitude versus frequency  $\omega$  is shown in Fig. 15. A very clear and pronounced peak response is observed at a frequency of 6.67 Hz compared with the measured frequency of 6.5 Hz. The computed dynamic stiffnesses of the single pile at  $f = 6.67$  Hz are  $k_{vv} = 1.34 \times 10^5$  kN/m,  $k_{v\theta} = -1.31 \times 10^5$  kN/rad, and  $k_{\theta\theta} = 2.0 \times 10^5$  kN·m/rad. The computed and measured frequencies and damping ratios for the translation and vertical modes of response are given in Table 1.

The computed and measured frequencies of peak response agree very well. The computed pile head damping ratio for the horizontal mode is somewhat higher than the measured damping ratio. This is probably due to the fact that the analysis is elastic and the hysteretic damping corresponding to low-strain behaviour of the real soil had to be selected by judgement.

**Free vibration test on a pile-supported transformer: six-pile group**

To verify the applicability of the proposed model for the analysis of pile groups, the proposed quasi-3D finite element method has been used to analyze a free-vibration test on a six-pile group. A quick release horizontal vibration test was performed on a full-scale pile group foundation of a large transformer bank (Bank 79) located at the Duwamish Substation, Seattle, Washington. Test data and analytical results were reported by Crouse and Cheang (1987). The foundation of the transformer bank consists of a pile cap with six vertical piles embedded in 12.20 m of loose saturated, sandy soils overlying stiff soil.

**Fig. 16.** Idealized soil profile at Duwamish Substation (modified from Crouse and Cheang (1987)).

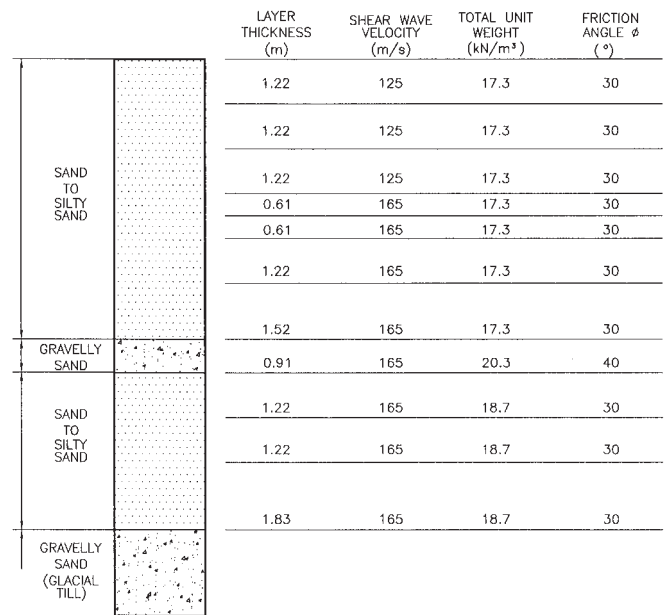


**Table 1.** Computed and measured resonant frequencies and damping ratios of the Franki pile foundation.

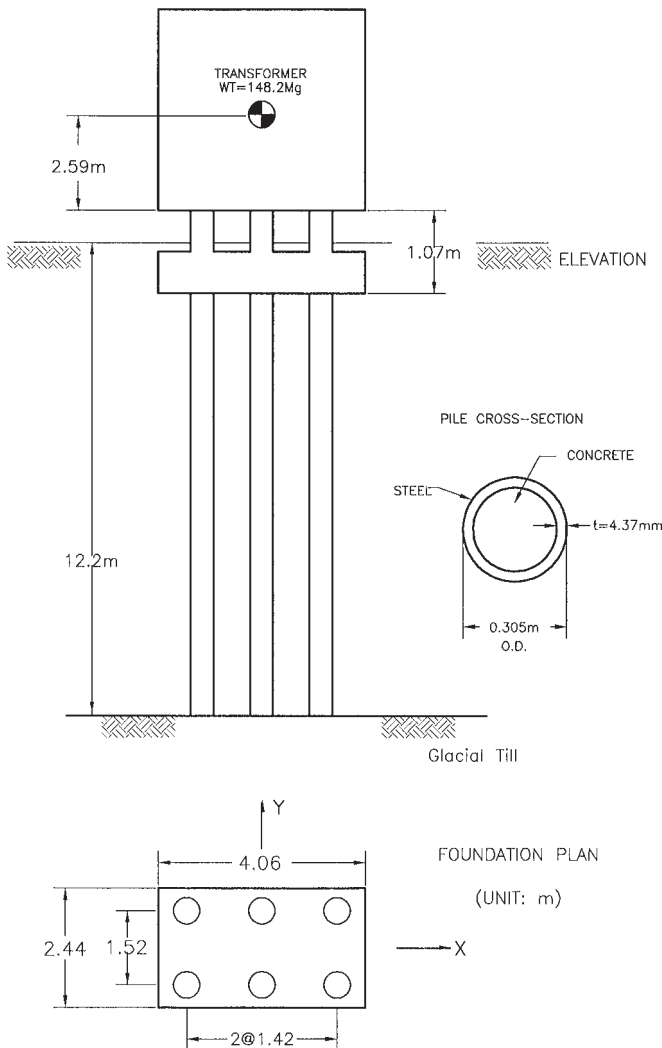
Mode of excitation	Computed resonant frequency (Hz)	Measured resonant frequency (Hz)	Computed damping ratio	Measured damping ratio
Vertical	44.0	46.5	0.04	0.05
Translational	6.67	6.50	0.06	0.04

The soil profile at the location of the transformer bank consists of mostly loose to medium dense sand to silty sand, with some dense sand or gravelly sand layers, overlying very dense gravelly sand (glacial till) at 12.2 m depth. The ground-water table was at a depth of 3.7 m. The in situ shear wave velocities ( $V_s$ ) measured from a downhole seismic survey in the sand to silty sand deposits are 125 m/s in the upper 3.7 m and 165 m/s below 3.7 m depth. Figure 16 shows the idealized soil profile at Duwamish Station according to Crouse and Cheang (1987).

Figure 17 shows the transformer bank and the pile foundation. The transformer, weighing 1454.0 kN is anchored to a concrete pedestal, which is a continuous part of the pile cap. The pile cap with dimensions of 4.06 m by 2.44 m is embedded beneath the ground surface, as shown in Fig. 17. The pile foundation consists of six vertical concrete-filled steel pipe piles, 0.305 m outside diameter with 4.37 mm wall thickness. These piles are spaced at 1.42 and 1.52 m centre to centre in the  $X$  and  $Y$  directions, respectively. All the piles are extended into the very dense glacial till layer at 12.20 m depth. The composite compressional rigidity ( $EA$ ) and the flexural rigidity ( $EI$ ) of each concrete-filled pipe pile are  $2.27 \times 10^6$  kN and 2034.46 kN·m<sup>2</sup>, respectively, where  $E$  is Young's modulus,  $A$  is the cross-sectional area, and  $I$  is the bending moment of inertia.



**Fig. 17.** Setup of a full-scale free vibration test on a six-pile group (modified from Crouse and Cheang (1987)).

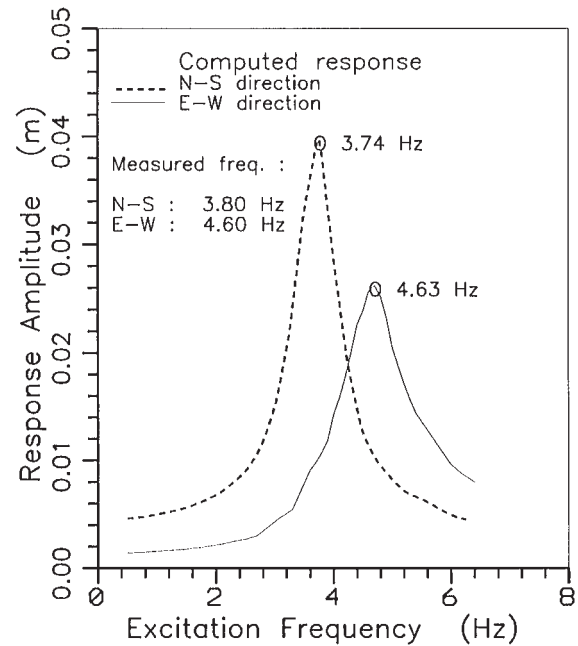


According to Crouse and Cheang (1987), the measured fundamental frequencies in north-south ( $Y$  axis) and east-west ( $X$  axis) directions are 3.8 Hz and 4.6 Hz, respectively. The measured damping ratios in the north-south and east-west directions are 6% and 5%, respectively.

In the present analysis, the soil profile shown in Fig. 16 is used except that the shear modulus distribution as modified by Sy (1992) is adopted. According to Sy (1992), a correction based on measured shear wave velocity was made to account for the soil densification due to pile installation. An increase of 4% in low strain shear modulus  $G_{max}$  values was applied to the measured free field values for this correction. Poisson's ratio  $\mu = 0.3$  and material damping ratio  $\lambda = 5\%$  are used for all soil layers in present analysis. Radiation damping was also included.

Dynamic impedances of the six-pile group, ignoring pile cap embedment, were computed first using the proposed model. Then the dynamic impedances due to pile cap embedment were evaluated. In the embedment analysis, only the soil reactions acting on the vertical sides of the pile cap were included and the soil reactions acting on the base of the pile cap were not considered. This procedure was justified on the basis

**Fig. 18.** Computed response curves of the transformer – pile cap system for determination of resonant frequencies.



that gaps between the pile cap and the soil underneath it may exist due to settlement of soil (Crouse and Cheang 1987). Conventionally the effect of pile cap – soil interaction is usually included by considering only the soil reaction acting on the vertical sides of the pile cap (Prakash and Sharma 1990; and Novak et al. 1990). The side reaction usually results in increased foundation stiffness and damping. Beredugo and Novak (1972) determined the foundation stiffness and damping due to pile cap embedment using a plain strain soil model that included only the soil reaction against the vertical face of the cap.

The rectangular pile cap had an area of 9.91 m<sup>2</sup> and an equivalent radius of 1.776 m. The embedment depth of the pile cap was 0.534 m, and the shear modulus of soil at that depth was 28 790 kPa. Based on these data, using Beredugo and Novak's solution, the stiffness and damping due to pile cap embedment were determined at the bottom of the pile cap to be  $k_{vv}^* = 61\,441.0$  kN/m,  $C_{vv}^* = 1945.63 \omega$  kN/m;  $k_{v\theta}^* = 16\,412.80$  kN/rad,  $C_{v\theta}^* = 517.36 \omega$  kN/rad; and  $k_{\theta\theta}^* = 127\,000$  kN·m/rad,  $C_{\theta\theta}^* = 1400.5 \omega$  kN·m/rad.

The total stiffness and damping factors of the transformer foundation, obtained by adding the stiffness and damping due to pile cap embedment to those of the six-pile group, are shown in Table 2 at the resonant frequencies for each direction of shaking.

To determine the resonant frequencies of the transformer – pile cap system, the dynamic response of the system is computed by subjecting the system to horizontal harmonic forced excitation at different frequencies. Harmonic force and moment were applied at the centre of gravity of the transformer – pile cap system. According to Crouse and Cheang, the transformer and pile cap have a total mass of 165.30 Mg. The height of centre of gravity of the system is 3.323 m above the pile head. The moments of inertia are 595.57 and 742.43 Mg·m<sup>2</sup> about axes in the north-south direction and in the east-west direction, respectively. The computed combined dynamic impedance of the six-pile group and the pile cap embedment are attached to

**Table 2.** Computed stiffness and damping factors of the transformer pile foundations including the effect of pile cap embedment.

	NS direction ( $f = 3.74$ Hz)	EW direction ( $f = 4.63$ Hz)
$k_{vv}$ (kN/m)	$3.60 \times 10^5$	$3.73 \times 10^5$
$k_{v\theta}$ (kN/rad)	$-0.99 \times 10^5$	$-1.08 \times 10^5$
$k_{\theta\theta}^{\text{cap}}$ (kN·m/rad)	$1.82 \times 10^6$	$3.52 \times 10^6$
$C_{vv}$ (kN/m)	$1.46 \times 10^5$	$1.29 \times 10^5$
$C_{v\theta}$ (kN/rad)	$-2.27 \times 10^4$	$-0.88 \times 10^4$
$C_{\theta\theta}^{\text{cap}}$ (kN·m/rad)	$1.25 \times 10^5$	$2.36 \times 10^5$

Note: NS, north–south; EW, east–west.

**Table 3.** Measured and computed resonant frequencies and damping ratios including the effect of pile cap embedment.

Natural frequencies ( Hz)				Damping ratios			
Computed		Measured		Computed		Measured	
NS	EW	NS	EW	NS	EW	NS	EW
3.74	4.63	3.80	4.60	0.09	0.09	0.06	0.05

Note: NS, north–south; EW, east–west.

the base of the transformer – pile cap system as springs and dashpots.

Figure 18 shows the response curves of the transformer-pile cap system when the effect of pile cap embedment is included. The computed resonant frequencies and damping ratios of the transformer – pile cap system are determined from Fig. 18.

The computed resonant frequencies and damping ratios, including the effect of pile cap embedment, are compared with the measured data in Table 3. The computed resonant frequencies match very well with the measured frequencies in both principal directions. However, the computed damping ratios are higher than the measured damping ratios.

## Summary and discussion

A quasi-3D finite element method of analysis has been presented for dynamic response analysis of single piles and pile groups. The proposed method is based on a simplified 3D wave equation for describing the dynamic response of foundation soils. The use of the quasi-3D method of analysis greatly reduces computer RAM requirements and the CPU time required for the analysis. Thus the method makes direct dynamic analysis of pile foundations involving large pile groups computationally feasible. The verification studies indicate that, under damped linear elastic conditions, the proposed quasi-3D method does indeed produce solutions that are in good agreement with the existing elastic solutions, such as those by Kaynia and Kausel (1982) and Novak et al. (1990) and with results of full-scale low amplitude field vibration tests on a single pile and a six-pile group. The method is extended to analysis of nonlinear soil response in the accompanying paper by Wu and Finn (1997).

## Acknowledgement

The postgraduate fellowship awarded by the Natural Sciences

and Engineering Research Council of Canada (NSERC) to the first author is acknowledged. This work was also supported in part by grant from NSERC to the second author.

## References

- Beredugo, Y.O., and Novak, M. 1972. Coupled horizontal and rocking vibration of embedded footings. *Canadian Geotechnical Journal*, **9**: 477–497.
- Crouse, C.B., and Cheang, L. 1987. Dynamic testing and analysis of pile-group foundations. *In* Dynamic response of pile foundations—experiment, analysis and observation. American Society of Civil Engineers, Geotechnical Special Publication No. 11, pp. 79–98.
- Fan, K., Gazetas, G., Kaynia, A., Kausel, E., and Ahmad, S. 1991. Kinematic seismic response of single piles and pile groups. *Journal of Geotechnical Engineering*, ASCE, **117**: 1860–1879.
- Finn, W.D.L., and Wu, G. 1994. Recent developments in dynamic analysis of piles. *Proceedings of the 9th Japan Conference on Earthquake Engineering*, Tokyo, Vol. 3, pp. 325–330.
- Gazetas, G. 1984. Seismic response of end-bearing piles. *Soil Dynamics and Earthquake Engineering*, **3**: 82–94.
- Gazetas, G., Fan, K., and Kaynia, A. 1993. Dynamic response of pile groups with different configurations. *Soil Dynamics and Earthquake Engineering*, **12**: 239–257.
- Kaynia, A.M., and Kausel, E. 1982. Dynamic stiffnesses and seismic response of pile groups. Department of Civil Engineering, Massachusetts Institute of Technology, Cambridge, Report R 82–03.
- Novak, M. 1974. Dynamic stiffness and damping of piles. *Canadian Geotechnical Journal*, **11**: 574–598.
- Novak, M. 1991. Piles under dynamic loads. *Proceedings, State of the Art Paper, 2nd International Conference on Recent Advances in Geotechnical Earthquake Engineering and Soil Dynamics*, University of Missouri–Rolla, Rolla, Vol. III, pp. 250–273.
- Novak, M., and Aboul-Ella, F. 1978. Impedance functions of piles in layered media. *ASCE Journal of Engineering Mechanics*, **104**: 643–661.
- Novak, M., Sheta, M., El-Hifnawy, L., El-Marsafawi, H., and Ramadan, O. 1990. DYN3: A computer program for calculation of foundation response to dynamic loads. Geotechnical Research Centre, the University of Western Ontario, London.
- Prakash, S., and Sharma, H.D. 1990. *Pile foundation in engineering practice*. John Wiley & Sons, Inc., New York.
- Sy, A. 1992. An alternative analysis of vibration tests on two pile group foundations. *Piles under dynamic loads*, American Society of Civil Engineers, Geotechnical Special Publication No. 34, pp. 136–152.
- Sy, A., and Siu, D. 1992. Forced vibration testing of an expanded base concrete pile. *In* Piles under dynamic loads. American Society of Civil Engineers, Geotechnical Special Publication No. 34, pp. 170–186.
- Wu, G. 1994. Dynamic soil-structure interaction: Pile foundations and retaining structures. Ph.D. thesis, Department of Civil Engineering, The University of British Columbia, Vancouver.
- Wu, G., and Finn, W.D.L. 1995. A new method for dynamic analysis of pile groups. *Proceedings, 7th International Conference on Soil Dynamics and Earthquake Engineering*, Crete, Greece, May 24–26, 1995, Vol. 7, pp. 467–474.
- Wu, G., and Finn, W.D.L. 1996. Seismic pressures against rigid walls. *Analysis and Design of Retaining Structures Against Earthquakes*. American Society of Civil Engineers Convention, Washington, D.C., November.
- Wu, G., and Finn, W.D.L. 1997. Dynamic nonlinear analysis of pile foundations using finite element method in the time domain. *Canadian Geotechnical Journal*, **34**: 44–52.